1-1-2022

Bottom-Up versus Top-Down Strategies for Morphology Control in Polymer-Based Biomedical Materials

Alexander B. Cook
Istituto Italiano di Tecnologia, a.b.cook@tue.nl

Tristan D. Clemons
University of Southern Mississippi, Tristan.Clemons@usm.edu

REVIEW

ADVANCED
NANOBIOMED
RESEARCH
Open Access

www.advnanobiomedres.com

Bottom-Up versus Top-Down Strategies for Morphology Control in Polymer-Based Biomedical Materials

Alexander B. Cook* and Tristan D. Clemons*

The size and shape of polymer materials is becoming an increasingly important property in accessing new functions and applications of nano-/microparticles in many scientific fields. New synthetic methods have allowed unprecedented capability for the facile fabrication of anisotropic and shape-defined nanomaterials. Bottom-up approaches including: emulsion polymerization techniques, amphiphile self-assembly, and polymerization-induced self-assembly, can lead to polymer particles with precise dimensions in the nanoscale. Top-down methods such as lithographic templating, and 3D printing, have increased the access to unique particle shapes. In this review, these recent developments are appraised and contrasted, with future research directions providing that focus on biomedical applications. Finally, the opportunity available for synergistic combinations of top-down and bottom-up fabrication approaches in realizing previously unattainable architectures and material properties is highlighted.

1. Introduction

The range of nano- or microengineered materials used in biological applications has increased dramatically over recent decades.[1–4] This increase in diversity of materials driven by synthetic chemistry advances and manufacturing insights, has led to the development of biomaterials and drug delivery formulations with precise size and shapes.[5,6] Many natural spherical and nonspherical anisotropic systems such as

A. B. Cook[+]
Laboratory of Nanotechnology for Precision Medicine
Istituto Italiano di Tecnologia
Via Morego 30, Genova 16163, Italy
E-mail: a.b.cook@tue.nl

T. D. Clemons
School of Polymer Science and Engineering
University of Southern Mississippi
Hattiesburg, MS 39406, USA
E-mail: tristan.clemons@usm.edu

The ORCID identification number(s) for the author(s) of this article can be found under https://doi.org/10.1002/anbr.202100087.

[+]Present address: Department of Chemical Engineering and Chemistry, Eindhoven University of Technology, Eindhoven 5600 MB, The Netherlands

platelets, tubulin, various viruses, mitochondria, and exosomes, all have certain physiochemical characteristics which facilitate function and the undertaking of unique biological tasks. Taking inspiration from these natural systems, researchers have identified size and shape parameters of critical importance in the engineering of new synthetic nanoparticles and materials to mimic these functions including, altered biodistribution to favour accumulation in certain organs, increase uptake into cells, and modulate response from the immune system among many others.[5,7,8]

The rational design of material morphology for biomedical applications can be achieved through the broad definitions of top-down or bottom-up synthetic strategies. In top-down fabrication methods, researchers aim to target material properties required for anticipated biological function such as overcoming certain intra or extra cellular biological barriers. Harnessing engineering techniques such as template lithography, flow lithography techniques, or precise stereolithographic 3D printing methods then allow for the replication of these material parameters.[9] One benefit of top-down design is that the materials produced have easily interchangeable variables, including: polymer composition used in particle fabrication, size and shape of the formed particles, and the active drug or imaging agents encapsulated. This allows for the straightforward study of particle structure–activity relationships, or targeting of different pathologies and diseases. However, top-down particle fabrication technologies can be difficult to scale to larger production without considerable process development expertise. Bottom-up particles can be engineered through self-assembly of amphiphilic lipids or macromolecules, into nano-objects of various morphologies primarily governed by the volume fractions of the component amphiphiles, as originally described by Israelachvili et al.[10–13] These self-assembly methods can be simple to scale up, can achieve control over particle internal structure, but can have limitations with regards to the range of shapes or morphologies accessible and can be highly susceptible to processing conditions (pH, solvent, temperature, and salt).

The basis for the emphasis on particle size and shape, is due to it being established as a key factor in several interactions which determine biological efficacy (highlighted graphically in **Figure 1**). Researchers have demonstrated that circulation time and biodistribution is greatly affected by particle morphology.[14,15] Cell uptake kinetics and also mechanisms are both
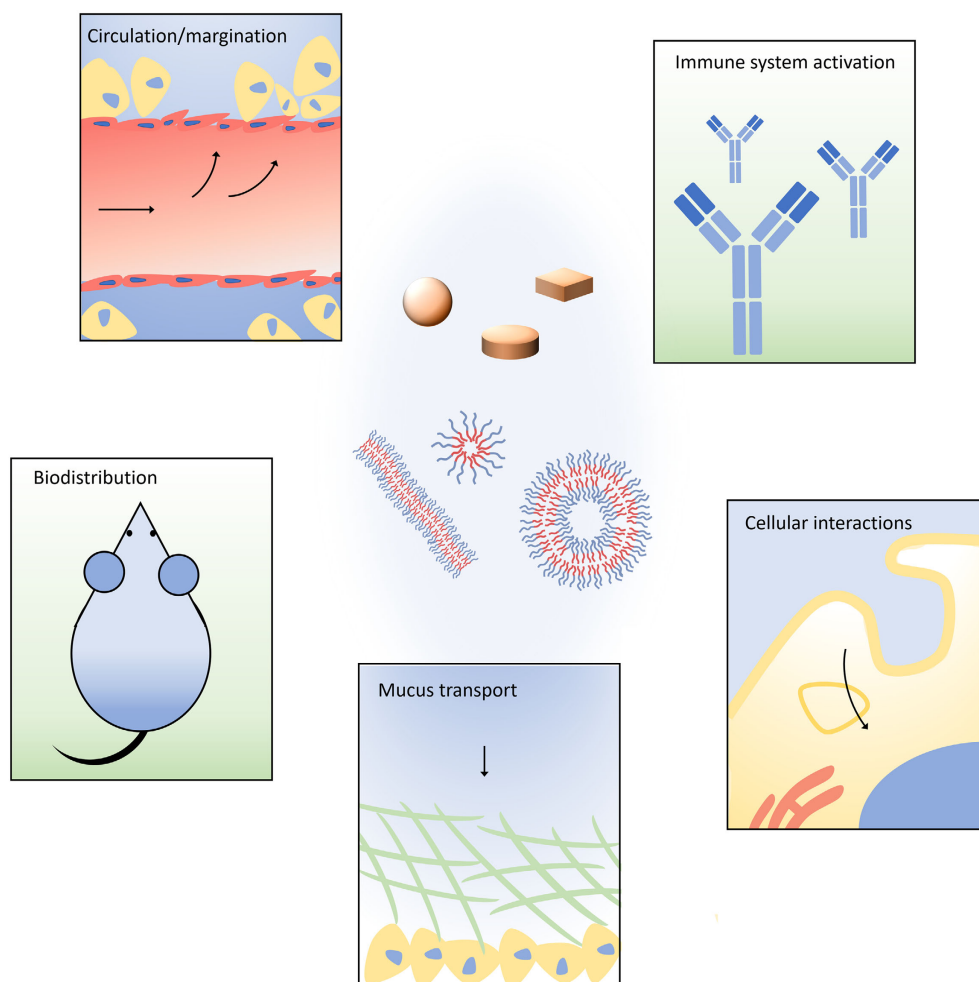
Figure 1. Material characteristics such as size, shape, surface charge, and chemical functionality can alter a wide range of interactions at the interface with biological systems. Design parameters can affect circulation, immune system activation, specific cell surface, and internalization pathways, mucosal transport, and biodistribution.

dependent on nanoparticle shape.[16,17] Additional effects such as vasculature margination of intravenously injected particles also play a role in the efficacy of nanomedicines.[18]

This review will focus on recent advances in the methods utilized to produce nanomaterials with tailored size and shapes for biomedical applications. First, the review will focus on bottom-up approaches, including emulsions and emulsion polymerization methods, the self-assembly of amphiphiles under specific temperature/pH/solvent/salt conditions to give nano- and microparticles with controlled morphologies, and biomedical applications of polymerization-induced self-assembly (PISA). Contrasting top-down approaches to the fabrication of materials with precise morphologies will then be presented, such as template-based lithography techniques, flow lithography methods, and recent 3D-printing-based advances. We believe, significant opportunity exists for multicomponent systems resulting from the combination of bottom-up and top-down strategies in the synthesis of hierarchical multicomponent systems with unique morphologies. In conclusion, we provide an insight into the challenges and opportunities possible through combining

these synthetic approaches, while providing a glimpse of future directions for the application of precise size- and shape-defined materials in biological contexts.

2. Bottom-Up Fabrication Approaches

Synthesis of anisotropic nanoparticles and biomaterials from the bottom-up assembly of lipids, peptide amphiphiles (PAs), or block copolymers, can allow access to smaller nanoscale dimensions and control of internal particle structure. Combining these self-assembly approaches with multiple immiscible phases can also allow access to intriguing morphologies of hierarchical droplets/particles, or janus particles with distinct patches of different functionalities. This section discusses recent advances in bottom-up self-assembly approaches, and the opportunities these provide for biomedical applications including therapeutic delivery and regenerative medicine. A summary of the bottom-up synthetic strategies covered in this review are shown in **Figure 2**.
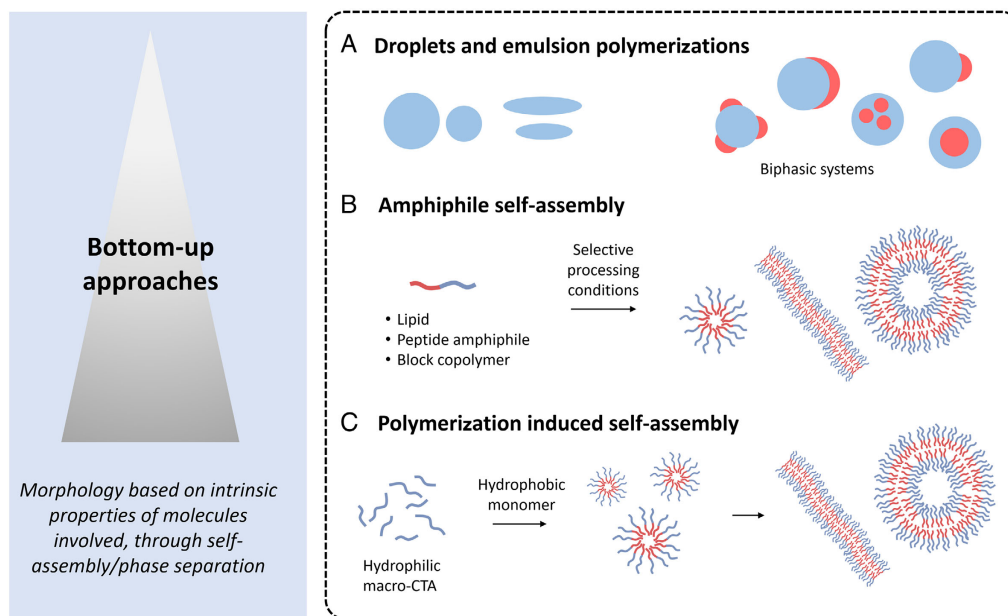
Figure 2. Bottom-up approaches to the formation of size- and shape-defined nanoparticles and microparticles, A) Emulsions and emulsion polymerizations, in single phases and with immiscible phases, B) Self-assembly of molecularly distinct amphiphiles with controlled conditions leading to morphologies of defined sizes and shapes. C) PISA of hydrophilic and hydrophobic monomers with reversible activation–deactivation radical polymerizations or controlled ring opening polymerizations.

2.1. Emulsions and Droplets

Emulsion polymerization is a facile and highly adopted synthetic approach for the formation of particles on the nano- to micrometer length scales.[19] Particles can be formed with a range of functional monomers, but the shape is often limited to spheres.[20,21] However, spherical polymer particles can be manipulated into anisotropic shapes such as ellipsoids with different aspect ratios, and disks, through careful control of temperature and solvents combined with the shear forces of strong stirring or film stretching.[22–24] These approaches to modify particle shape, pioneered by Mitragotri, has led to many insights into the impact nanoparticle shape has on cell phagocytosis, with local tangential angles determining the complexity of the actin structures formed during phagocytosis and ultimately whether the particle is internalized or not.[22] Another notable application of these shape-defined particles has been in the field of blood–brain barrier drug delivery.[25,26] The Mitragotri and coworkers have found that for the treatment of brain diseases, not only are the size and shape of formulations important factors due to endothelium margination, but also the mechanical stiffness of particles can greatly affect their interaction with the endothelium and transport through a cell monolayer.[25]

Droplets of coacervates or other polymer-containing solutions are being increasingly investigated as compartmentalized cell-mimicking systems.[27,28] In addition, microfluidic devices have been used as tools to create complex droplet in droplet morphologies, as shown in Figure 2.[29–31] Researchers can also form patchy particle morphologies though including different proportions of surfactants with phase separating polymer droplets, or sequential emulsion polymerization steps.[32–35] This formation of patchy particle morphologies can allow control over their

subsequent self-assembly into superstructures such as long filaments of particles, and thus allow further mimicking of biological processes and natural tissues.

2.2. Amphiphile Self-Assembly

The self-assembly of amphiphilic small molecules into larger nano-objects or hierarchical materials has been a consistent hallmark of bottom-up self-assembly methodologies. The self-assembly of lipid amphiphiles are integral for life through the assembly of phospholipids in our cell membranes regulating many biological processes. Most recently, the self-assembly of lipid nanoparticles were integral for the protection and packaging of vaccines against SARS-CoV-2, the virus responsible for the COVID19 global pandemic.[36,37] Through understanding the self-assembly phenomena of lipid amphiphiles, researchers have been able to design multicomponent systems, consisting of native biomembrane components, that can mimic cellular structures and processes.[38] Through precise control of lipid properties, pH, salt, solvent, and processing conditions, it is possible to achieve a range of architectures through lipid self-assembly including tubes,[39] cones,[40] bicelles,[41] giant vesicles,[42] and cisternae stacks.[41]

Often the self-assembly of amphiphilic molecules results in nanoassemblies which are inherently fragile resulting from their noncovalent interactions allowing for molecular mobility within, and exchange of molecules between assemblies.[43] Further, because of this dynamic molecular exchange, these assemblies often result in dissociation upon drying making them difficult to utilize in dry or bulk macroscopic material applications. Recent work from the Ortony lab aimed to address this with the development of a kevlar inspired, aramid amphiphile.[44] Due to strong anisotropic interactions among the aramid

amphiphiles, molecular exchange is significantly suppressed to allow for the spontaneous formation of long nanoribbons, with impressive mechanical properties (Young's modulus of 1.7 GPa and tensile strength of 1.9 GPa).[44] Further, the aramid amphiphile nanoribbons could be shear aligned and dried into threads which could support two hundred times their weight, providing an exciting example of the opportunity for the bottom-up synthesis of high-strength macroscopic materials.

The lively dynamics of molecules in amphiphile self-assembly also provides opportunities for unique material properties unattainable with covalent counterparts. PAs, consisting of an alkyl tail attached to charged peptide residues to provide molecular amphilicity, provide an ideal platform for exploring the opportunities molecular dynamic exchange can provide.[45,46] In an aqueous environment, aggregation of the aliphatic alkyl tails coupled with intermolecular hydrogen bonding among the peptide segments drive these molecules to form anisotropic architectures which can extend to many micrometer in length.[47] Recent work from the Stupp laboratory has demonstrated the ability to tune the molecular exchange of PA molecules in assemblies to drive the spontaneous assembly of hierarchical superstructures for dynamic material properties.[48–50] In fact, it has been demonstrated by both coarse-grained simulation and through recent experimentation that as long as the strength of noncovalent interactions among monomers in the PA self-assembly is low enough to allow monomers to escape from their original assemblies (dynamic molecular exchange), then there is potential for the formation of hierarchical superstructures.[49]

In a study by Edelbrock et al., PA molecules were designed to contain β-cyclodextrin and adamantyl moieties on the surface of PA nanoribbon assemblies that could form noncovalent host–guest inclusion complexes between molecules. When these host- and guest-functionalized nanoribbons were mixed, even at low concentrations of the functionalized molecules (10 mol% in their respective nanoribbons with 90 mol% unfunctionalized PA molecules), bundled superstructures of nanoribbons were observed. This superstructure was driven by the formation of host–guest inclusion complexes, and more importantly, the ability for these molecules to escape their original assemblies and enrich in the superstructure bundles (**Figure 3**A–C).[48] When the intermolecular cohesive energy of the PA molecules was increased, through the addition of hydrophobic amino acids that favor
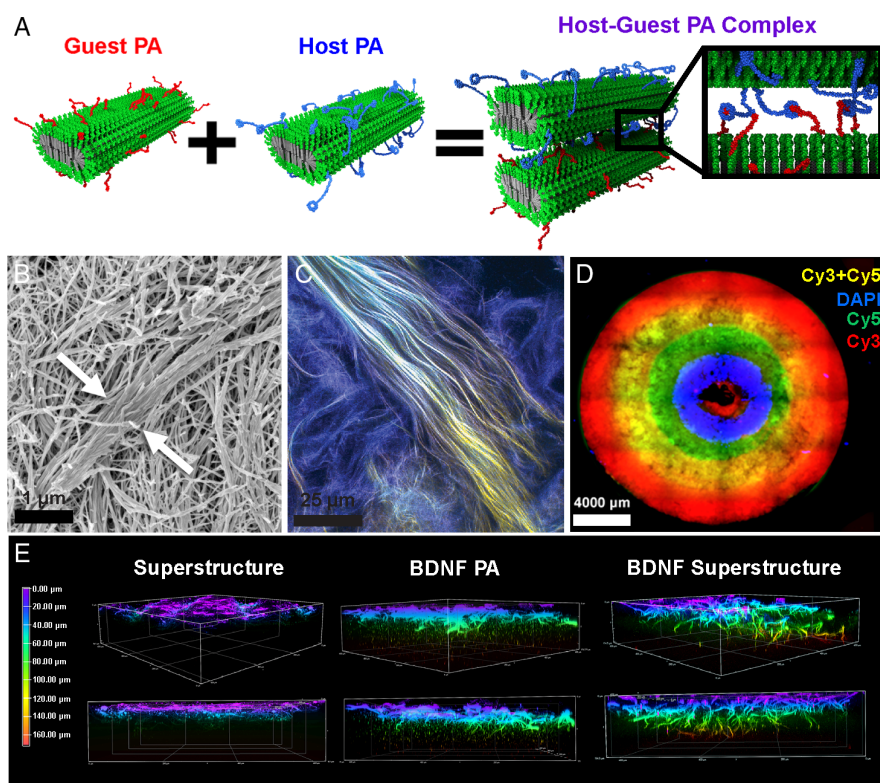

Figure 3. Harnessing dynamic molecular exchange in PA self-assembling nanoribbons for hierarchical superstructure formation. A) Schematic representation of the formation of host and guest inclusion complexes between functional groups in PA nanoribbons. B) Scanning electron microscopy (SEM) micrograph of the bundled superstructure formation. C) Confocal microscopy micrograph of the bundled superstructure formation between nanoribbons labeled with fluorescent dyes for visualization (guest PA (Cy3, red) and host PA (Cy5 dye, green)) coassembled with an unfunctionalized diluent PA (DyLight 405 dye, blue). Note the distinct yellow in the superstructured bundle resulting from enrichment of the host- (red) and guest- (green) functionalized molecules. D) Wide-field fluorescence microscopy micrograph of a 3D-printed concentric circle architecture as a demonstration of the ability to print well-defined brain mimetic architectures with the superstructured hydrogel. E) Depth coded z-stack reconstructions showing neuron infiltration on the superstructure, the BDNF mimetic PA, and the BDNF PA combined with the superstructure after 7 days in vitro. Neurons demonstrated the greatest infiltration when the bioactive BDNF mimetic peptide sequence was combined with the increased porosity resulting from the superstructure self-assembly. Reproduced under the terms and conditions of the Creative Commons Attribution license 4.0.[48] Copyright 2021, The Authors, published by Wiley-VCH.

intermolecular hydrogen bonding within the nanoribbons, molecular exchange was suppressed and superstructure formation was not observed. The formation of this bundled nanoribbon superstructure drastically increased the mechanical capabilities of the hydrogel, resulting in a highly porous architecture that was amenable to 3D bioprinting (Figure 3D). Further, functionalization of the porous superstructured material with a biological signal designed to mimic the important neuronal growth factor brain-derived neurotrophic factor (BDNF) produced a matrix with significant in vitro bioactivity. Neuron maturation and penetration into the hydrogel was enhanced as a result of this bioactive BDNF mimetic signal being coupled with the increased hydrogel porosity resulting from the self-assembly-driven superstructure formation (Figure 3E).[48] This work provides an example of the beneficial role dynamic molecular exchange in assemblies can play in the design of novel biomaterials, an opportunity unique to self-assembling systems and bottom-up synthetic pathways.

Extending from the self-assembly of lipid- and peptide-based amphiphiles, amphiphilic block copolymers can similarly assemble into multiple distinct morphologies. One advantage of using synthetic polymers here, is the ability to easily change the functionality of the monomers, or the length of the corresponding polymer blocks to alter the self-assembly properties. Shapes can range from spherical micelles and elongated tubular micelles of different lengths,[51,52] to larger diameter spherical polymersomes and the corresponding anisotropic tubular polymersomes.[16,53] One of the first examples demonstrating different biological effects of self-assembled polymer shape came from Discher and co-workers, who studied spherical micelles and tubular micelles of lengths from 2 to 18 μm.[51] The flexible tubular micelles had long circulation times in rodents of ≈1 week, compared with spheres of similar composition with circulation times an order of magnitude lower. Paclitaxel-loaded tubular micelles of 8 μm in length also demonstrated greater tumor growth inhibition when compared with the shorter 1 μm tubular micelles. A similar effect was seen by Larnaudie et al., with self-assembled nanotube structures formed from peptide polymer conjugates, where the anisotropic tubular nanostructures had longer circulation half-life compared with the individual polymer conjugates.[54]

Williams and co-workers have extensively studied tubular micelles and tubular polymersomes in biological systems.[55–57] Small micellular spheres and tube morphologies can be formed from block copolymers of poly(ethylene glycol) and poly(caprolactone-gradient-trimethylenecarbonate), PEG-*b*-p(CL-*g*-TMC), whereas larger polymersome spheres and tubes can be formed from block copolymers of PEG and poly(D,L-lactide), PEG-*b*-PDLLA.[55] With both polymer compositions, the tubular assemblies were found to have greater cell uptake compared with their corresponding sphere morphologies, for both sizes. While dexamethasone release was observed to be slower for the tubular structures. An ex vivo porcine eye model was used to assess the impact of shape on particle diffusion in biological media; increased mobility was observed for smaller and higher aspect ratio particles. This increase in mobility, resulting from controlling particle size and shape, will result in an increased number of particle–cell interactions and in turn supports the increased cellular uptake observed in vitro.[55,58] It has been found that block copolymer-based wormlike micelles have benefits for passively targeting inflamed mucosal tissue, in an ex vivo model of inflammatory bowel disease, due to their unique size and geometry.[59] Micelles penetrated both healthy and diseased tissue, whereas polymersomes penetrated neither due to their large diameters, and tubular micelles showed low up take in healthy colonic biopsies but increased ability to enter diseased human mucosa, demonstrating colocalization with immune cells.[59] These studies clearly demonstrate both the importance and opportunity possible with controlling polymer self-assembly morphology, especially with respect to anisotropic architectures in biology, for drug delivery and particle penetration.

2.3. Polymerization-Induced Self-Assembly

The polymer self-assembly of nanomaterials into a number of morphologies has attracted great attention due to their applications in many disciplines ranging from drug/gene delivery agents,[60] imaging contrast enhancers,[61] nanoreactors,[62] and surface coatings and catalysis.[63] However, traditional methods for self-assembly of polymeric nanomaterials are often conducted at low polymer concentrations (<1%) and regularly require some form of "triggering" for assembly such as pH modification or solvent exchange.[64] Resulting from these drawbacks, PISA has recently become a useful method to synthesize block copolymer nanomaterials in varying morphologies at high polymer concentrations (up to 50%).[64,65] In aqueous PISA, a water-soluble macromolecular initiator is used to polymerize relatively hydrophobic monomers to form amphiphilic diblock copolymers that self-assemble in situ, producing a range of morphologies and structures which evolve during the course of the polymerization (Figure 2C).[66,67] Recent progress in aqueous PISA is particularly exciting due to the synthesis of structures suitable for biological applications as well as the environmental and economic benefits of using green chemistry techniques through high atom efficiency, the use of aqueous media, and reduced purification requirements.[66,68]

A key requirement of the PISA process is the utilization of a controlled/living polymerization method to allow for efficient and predictable chain extension of the core-forming block. Reversible addition–fragmentation chain transfer (RAFT) polymerization, with the ability to produce precise molecular weight polymers, with low polydispersity, superb utility in aqueous systems, and suitability for a large range of monomer classes has been the polymerization method of choice for PISA systems.[64–67,69–71] In stating this, other controlled polymerization methods have also successfully been used to produce PISA nanoparticles including atom transfer radical polymerization (ATRP),[72–74] nitroxide-mediated radical polymerization (NMP),[75–78] living anionic polymerisation,[79] and ring opening metathesis polymerization (ROMP).[18,19,68,80,81] The main prerequisite is the ability to polymerize an insoluble polymer block from soluble monomers utilizing a macroinitiator in a specific antisolvent.[74] PISA is an exciting method for the production of polymeric nanomaterials at high solid content and has been utilized to realize a vast array of different morphologies (**Figure 4**),[67] however, typically micelles, rods, worms, and vesicles are observed.[82]

**ADVANCED
SCIENCE NEWS**

www.advancedsciencenews.com

**ADVANCED
NANOBIOMED
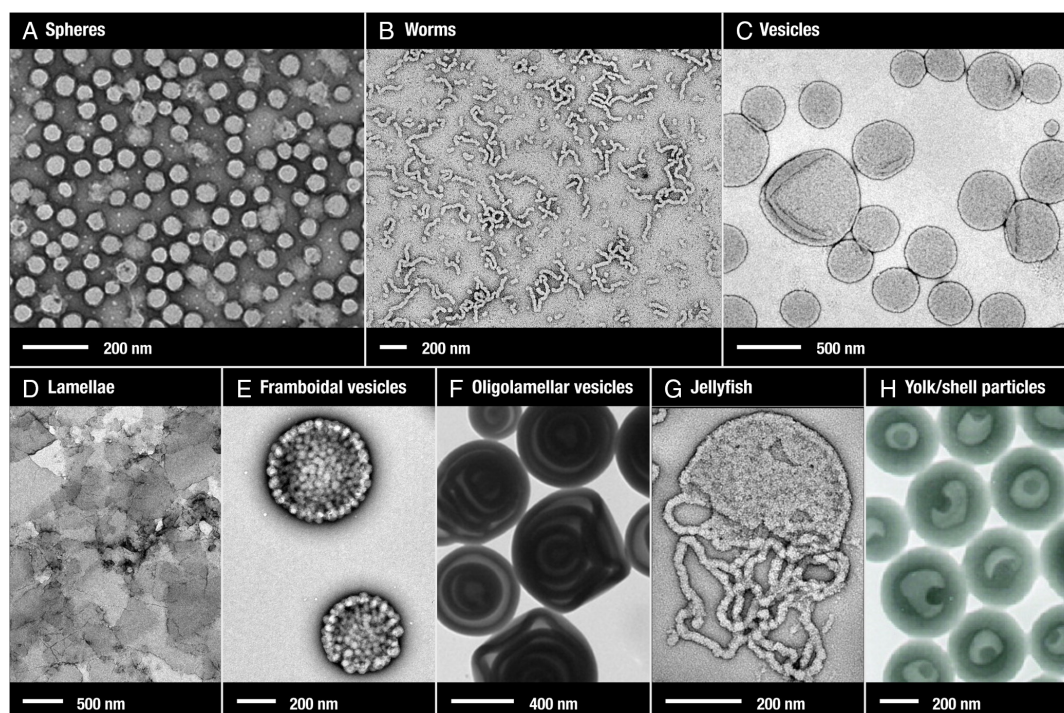RESEARCH**
Open Access

www.advnanobiomedres.com

Figure 4. Transmission electron micrographs of PISA a) spheres, b) worms, c) vesicles, d) lamellae, e) framboidal vesicles, f) oligolamellar vesicles, g) jellyfish, and h) yolk/shell particles. Reproduced under the terms and conditions of the Creative Commons Attribution CC-BY license.[67] Copyright 2016, American Chemical Society. Individual panels: a) Reproduced with permission.[132] Copyright 2013, American Chemical Society. b,c,g) Reproduced with permission.[133] Copyright 2011, American Chemical Society. d) Reproduced with permission.[134] Copyright 2013, American Chemical Society. e) Reproduced under the terms and conditions of the Creative Commons Attribution CC-BY license.[67] Copyright 2016, American Chemical Society. f) Reproduced with permission.[135] Copyright 2014, American Chemical Society. h) Reproduced with permission.[136] Copyright 2014, American Chemical Society.

The utility of PISA for controlling nanomaterial size and shape for biomedical applications was thoroughly reviewed by Davis and co-workers, in 2018,[11] hence in this section, we will provide a highlight of recent works making use of PISA for the synthesis of biomedical materials. PISA nanoparticles hold great promise as drug delivery vehicles; however, it is important to recognize the role incorporation of hydrophobic therapeutics may play in influencing the morphology of PISA assemblies. Recent work by Stenzel and co-workers investigated the influence of drug loading on the morphology of PISA nanomaterials and more importantly how this impacted biological function.[83] This work demonstrated that the inclusion of the model therapeutic curcumin during the PISA process, resulted in a shift in the phase diagram of expected morphologies. This change in observed morphologies, in turn impacted on nanoparticle cellular uptake and transport when assessed in multicellular spheroid models of cancerous solid tumours.[83] Gianneschi and co-workers utilized an aqueous, one-pot ring opening metathesis PISA (ROMPISA) synthesis for the development of a library of polymeric nanoparticles as cancer therapeutics.[84] This study investigated the role nanoparticle size, surface charge, and platinum loading had on the in vitro cytotoxicity of these nanoparticles with both human ovarian and cervical cancer cell lines. The same group also demonstrated the utility of the ROMPISA approach in the "open to air" synthesis of stimuli-responsive peptide polymer nanoparticles, which were able to spontaneously aggregate as a result

of treatments with a proteolytic enzyme.[85] These recent works demonstrates the utility of ROMPISA as a suitable method for achieving therapeutic nanoparticles, at high yields, in a one-step synthesis method.

The incorporation of peptides and PISA has garnered recent interest resulting from the opportunity peptides provide in both biorecognition and their propensity to drive self-assembly in attempts at influencing a wider array of morphologies available through PISA. Sun et al. successfully incorporated a proapoptotic peptide sequence (KLAKLAKKLAKLAK), previously demonstrated to induce rapid apoptosis of cancer cells through mitochondrial membrane disruption,[86] to display on the surface of PISA nanoparticles.[87] The one-pot synthetic approach allowed for facile tunability of both the therapeutic peptide loading on the surface of the nanoparticles as well as the nanoparticle size.[87] Interestingly, incorporation of this peptide on the surface of a polymeric nanoparticle resulted in increased proteolytic resistance of the therapeutic peptide and a significantly enhanced cellular uptake of the therapeutic nanoparticles resulting from the multivalent presentation of the KLA peptide. The group of Semsarilar and co-workers have also investigated several peptide–PISA-based systems aimed at incorporating self-assembling peptide motifs to support the formation of higher-order PISA morphologies driven by peptide self-assembly. In the first of these studies, a diphenylalanine peptide motif was copolymerized with glycerol monomethacrylate to create a

macro-CTA suitable for aqueous PISA with poly(2-hydroxypropyl methacrylate) as the core forming polymer.[88] In characterizing the subsequent nano-objects resulting from this approach, it was found that long anisotropic morphologies were observed, a result likely to have been achieved through the contributions of the peptide self-assembly to the PISA process.[88] In a follow up study, the same group assessed the effect that the incorporation of pendant hydrophobic self-assembling tripeptide sequences would have on the PISA process when incorporated into the core forming polymer block.[89] Again, it was observed that differences in the hydrophobicity of these pendant peptide units along with their self-assembling propensity resulted in morphological differences in the observed nano-objects resulting from the PISA process.[89]

Finally, the application of PISA to create well-defined nanoparticles for investigating biological interactions in model systems is also an important consideration for the translation of PISA nanoparticles to clinically relevant biomaterials. Vu et al. demonstrated the ability to compare PISA synthesized nanospheres, ranging from 40 to 150 nm with low dispersity's and a negative surface charge, in a microfluidic system aimed at modeling human blood flow in a microvasculature network (**Figure 5**).[90] In this work, they demonstrate that large PISA nanoparticles exhibited higher associations to B cells, monocytes, and neutrophils compared with their smaller counterparts.[90] Further, this work provides direct insight into the role nanoparticle size can play on potential application with small anionic PISA nanoparticles (≈40 nm) suitable for cancer drug delivery due to their minimal interactions with immune cells, whereas large PISA nanoparticles (≈150 nm) may be useful for vaccine delivery targeting B cells.[90]

3. Top-down Fabrication Approaches

Fabrication of particles through top-down approaches offer the benefits of more complex particle morphologies, but can come at the expense of size limitations due to the lithographic processes and substrates used (a summary of top-down synthetic methods is shown in **Figure 6**). Templating lithographic methods have been extensively used for patterning in electronics, and in soft lithography for microfluidic chip preparation,[91] but were adapted to be used as micrometer and submicrometer particle fabrication techniques around 2005.[92] In general, template-based methods involve preparation of a master template from silica with etching (or other porous inorganic materials),[93,94] and secondary templates formed from either polydimethylsiloxane (PDMS) or water-soluble sacrificial polyvinylalcohol templates, with particles being fabricated directly in the template pattern and subsequently collected.[95,96] The particle replication in nonwetting templates (PRINT) methodology was developed by the DeSimone and co-workers, and has allowed synthesis of polymeric nanoparticles of well-defined geometries from tens of nanometers to micrometers.[92] The group has investigated the role of particle shape on biodistribution and cell uptake in vivo with radio-labeled polyethylene glycol (PEG)-based particles of ≈200 nm in diameter.[97] It was found that high aspect ratio cylindrical rod-shaped particles had significantly increased internalization rates in HeLa cells compared with cylinders of the same cross section but with lower aspect ratios.[98] Decuzzi and co-workers have used imprint lithography to create a range of nano- and microparticles with a variety of shapes from square microplates, to disk-shaped particles, and have found that disk-shaped
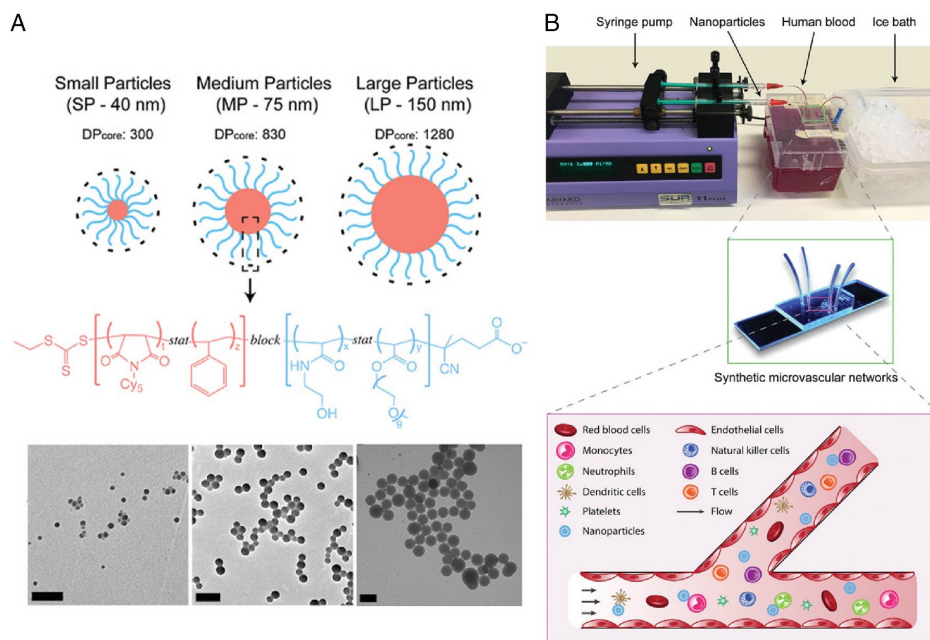

Figure 5. A) Top: Schematic illustration of nanoparticles prepared by RAFT PISA of three different sizes of ≈40 nm (small particle—SP), ≈75 nm (medium particle—MP), and ≈150 nm (large particle—LP); Middle: Chemical structure of diblock copolymers of the PISA nanoparticles; Bottom: Representative TEM images of the PISA nanoparticles B) Top: A photo of the human blood flow microvasculature mimetic setup. Middle: A synthetic microvascular network; Bottom: Schematic illustration of nanoparticle interactions with different cell types found in whole blood under flow conditions. Reproduced with permission.[90] Copyright 2020, Wiley-VCH.
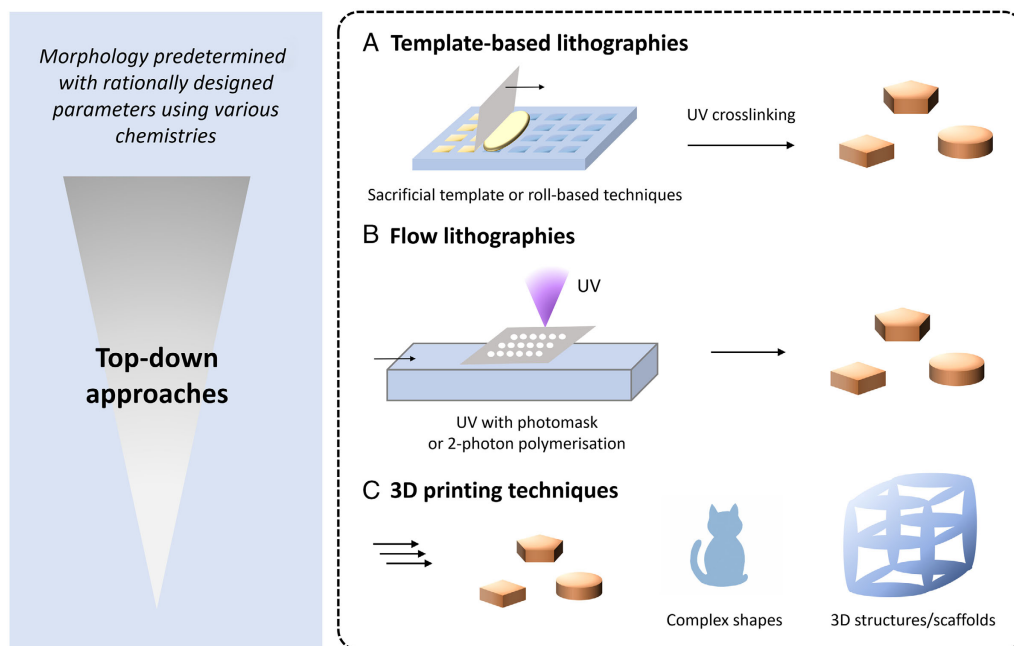
**ADVANCED
SCIENCE NEWS**

www.advancedsciencenews.com

**ADVANCED
NANOBIOMED
RESEARCH**
Open Access

www.advnanobiomedres.com

Figure 6. Top-down approaches to the formation of size- and shape-defined nanoparticles and microparticles. A) Template-based and imprint lithographic methods with either dissolvable sacrificial templates, or crosslinked reusable templates. B) Flow-based lithographic methods can incorporate UV light with shaped defined photomasks, or two photon polymerization. C) Stereolithography or 3D printing can offer the most diverse range of accessible morphologies of micro- and nanoparticles, however, is potentially less scalable.

particles offer advantages in vascular wall targeting similarly to erythrocytes.[99] The size of square and cube microplates of polylactic-*co*-glycolic acid (PLGA) was found to be a determining factor in the release of anti-inflammatory therapeutics such as curcumin and dexamethasone from the polymer carrier particles.[100] Hydrogel microparticles with anisotropic shapes have also been developed by De Laporte and co-workers, using a perfluoropolymer mold-based soft lithography approach, and ultraviolet (UV) light initiated crosslinking of PEG macromonomers.[101] By including superparamagnetic iron oxide nanoparticles (SPIONs) in the PEG phase during crosslinking, the anisotropic rod-shaped microgels can be aligned using an external magnetic field. The alignment of shape-defined particles has been used to help guide a variety of cells in 3D space and could allow for more tunable cell cultures and multicellular tissue constructs for regenerative medicine applications.

In contrast to mold-based templating lithographic methods, flow lithography can produce particles with precise morphologies at a potentially higher scalability, and were pioneered in microfluidic chips by Doyle and co-workers (**Figure 7**).[102] Typically researchers use UV light and a photomask engineered to let light pass in the shape of the desired particle, which initiates polymerization in a solution of particle precursors. The flowing solution of particle precursor can be continuous, or polymerized in stop-flow conditions.[102–104] Shapiro et al., used particle shape as a parameter to enhance the signal of protein-based assays of thyroid-stimulating hormone (TSH).[105] The authors found that the ratio of surface area to the 2D projection used for imaging, was key to lowering the limit of detection of the desired biomarkers. The increased surface area of ring-shaped and wheel-shaped

microparticles, compared with disk-shaped particles, increased the fluorescent signal twofold and the TSH limit of detection sixfold, respectively. Segmented illumination of flowing polymer precursors has also been developed to produce particles of differing sizes and shapes, in a high throughput manner.[106] The produced PEG-based microgel particles had tunable Young's moduli and could also be fabricated with a cell adhesive arginine-glycine-aspartic acid tripeptide (RGD) peptide-based acrylate incorporated into the hydrogel allowing for optimal biocompatibility.

Stereolithography or 3D printing is being increasingly used for the fabrication of biomedical materials with tailored shapes. In this review, which is primarily focused on micro- and nanoparticles, we will not consider larger macroscale scaffolds or bioprinting,[107] although 3D printing is widely used for these applications.[108] Complex shapes like helical particles have been used as microswimmers in nanomedicine applications, and access to these particle shapes can only be provided by 3D printing. Kraft and co-workers fabricated a range of particles, including helical particles, from two photon polymerization of propylene glycol methylether acrylate and sputter-coated sections of the particles to have catalytically active sites for self-propulsion.[109] The platinum/palladium coating could be applied to the end of the particles or the side, which altered the axis of directional motion compared with the main length axis of particles, but not the overall velocity. Sitti and co-workers have also fabricated helical microparticles as theranostic payload delivery systems (**Figure 8**).[110] The researchers used a rotating magnetic field to actuate the helices, and included iron oxide nanoparticles in the gelatin methacryloyl hydrogel for this purpose. Enzymatically controlled drug release from the microswimmers could be achieved in the presence of
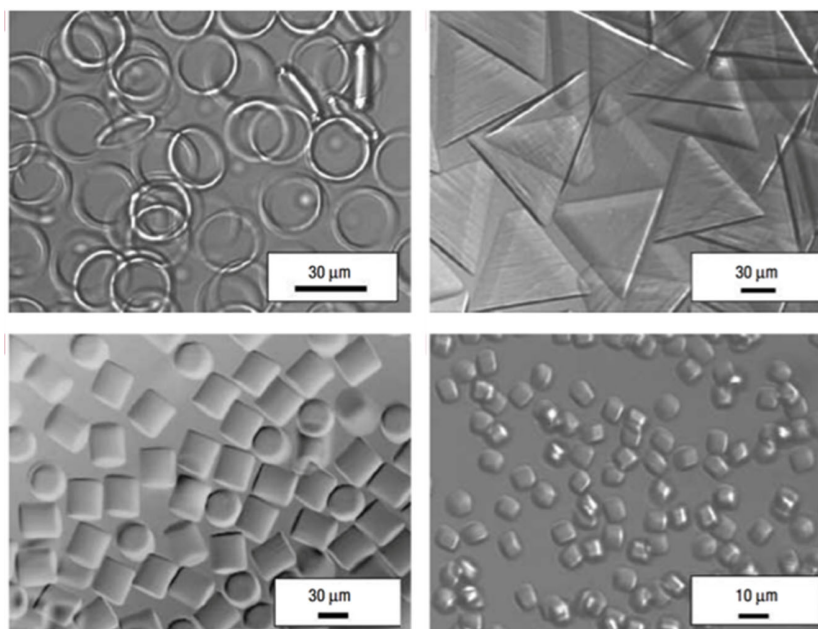
2100087 (8 of 14)

**ADVANCED
SCIENCE NEWS**

www.advancedsciencenews.com

**ADVANCED
NANOBIOMED
RESEARCH**

www.advnanobiomedres.com

Figure 7. Images of microparticles fabricated using high throughput continuous flow lithography of monomer solution, including rings, triangles, cylinders, and cuboid microparticles (differential interference contrast images). Reproduced with permission.[102] Copyright 2006, Springer Nature.
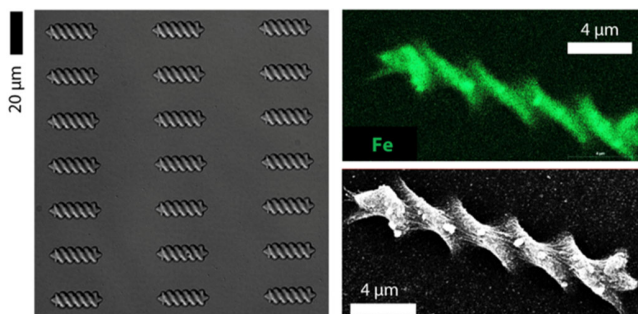

Figure 8. Images of 3D-printed biodegradable hydrogel microswimmers, including optical microscope differential interference contrast image, energy-dispersive X-ray spectroscopy iron elemental mapping, of the iron oxide magnetic particle components. Reproduced under the terms and conditions of the Creative Commons Attribution CC-BY license.[110] Copyright 2019, American Chemical Society.

matrix metalloproteinase-2 (MMP-2), with enzyme-dependent release rates achieved with varying concentrations of enzyme from 0.125 to 1 µg mL^{-1}.[110] Targeted delivery of active agents using microswimmers of precisely engineered size and shape could be an impactful area of biomedical research in the future—enabled by lithographic particle engineering. The size and shape of particles can also have a large impact on the body's immune response to introduced nanoparticles. The Moeller and co-workers investigated this with the 3D-printing of antigen nanoparticles for vaccine formulations.[111] Protein photoresists at a concentration of 40 wt% in buffer with photosensitizer (rose Bengal) were polymerized into various anisotropic particles with multiphoton lithography. Particles with the highest aspect ratio of 10, resulted in the greatest stimulation of RAW264.7 macrophages, with an

approximately tenfold increase in tumor necrosis factor alpha (TNF-α) secretion, relative to the particles with lower aspect ratios of 1 and 3.

4. New Synergistic Approaches Combining Both Bottom-Up and Top-Down Fabrication Methods

However, the general top-down and bottom-up strategies to fabricate materials with interesting size and shape characteristics have led to advances in our fundamental understanding of biological interactions with synthetic materials, both also have drawbacks. Top-down methods can have limited scalability, whereas bottom-up approaches have until recently had limited utility beyond spherical morphologies (a comparison of bottom-up and top-down fabrication methods advantages and disadvantages is shown in **Table 1**). A relatively unexplored avenue lies in the combination of techniques from both to form new structural motifs with higher-order complexity, providing a significant area for future research and discovery (**Figure 9**). A number of applications have already explored this idea, and will be highlighted here, including hierarchical particle in particle systems, Pickering emulsions with anisotropic particles, and the 3D printing of shape-defined particles, fibers, or droplets.

One way to combine the benefits of both approaches is through hierarchical particle in particle structures, where the carrier particle or loaded particles are fabricated from opposing top-down or bottom-up methods. There are a number of examples of this in the literature mostly involving spherical nanoparticles encapsulating in top-down microstructured particles, such as lithographically templated hydrogels, and 3D printed microparticles.[110,112,113] In another example, the Decuzzi and co-workers synthesized square PLGA microparticles encapsulating

2100087 (9 of 14)

Table 1. Comparison table of advantages and disadvantages of the discussed bottom-up and top-down materials fabrication methods.

|		Advantages	Disadvantages
Bottom-up	Emulsion-based	Fast, scalable, low-cost, multiple compartments possible	Limited to spheres (ellipsoids with film stretching)
	Amphiphile assembly	Mix and match components, functionality on surface, facile synthesis	Limited to spheres/worms/fibers/vesicles, structure and shape purity, optimization of assembly conditions
	PISA	Fast, scalable, low-cost, functionality on surface.	Limited to spheres/worms/fibers/vesicles, structure and shape purity, monomer and solvent limitations
Top-down	Templating lithography	Wide range of shapes, particle monodispersity	Water-soluble materials challenging, scalability challenging, nanoscale dimensions difficult
	Flow lithography	Potentially scalable with parallel devices, many shapes possible, water solubility	Limited control over polymerization depth, optimization of flow, and concentration parameters
	3D printing	Particle monodispersity, complex shapes and 3D networks possible	Limited monomer functionality and scalability is challenging
Combined methods	Pickering emulsions	Multiple compartments possible, multiple functionalities, interfacial interactions tunable with size/shape	Multistep preparation procedures, droplet shape limited to spheres (stabilizing particles tunable)
	Hierarchical particles-in-particles	Multiple compartments possible, multiple functionalities	Challenging characterization and scalability
	3D printing of particles	Spatial confinement of self-assembled structures, functional network formation, additional mechanical strength of printed material	Limited monomer functionality and scalability is challenging
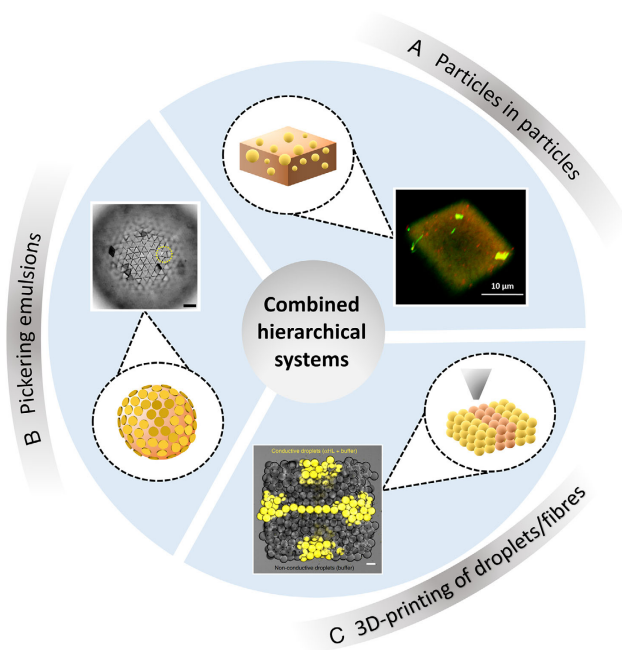
Figure 9. Combining top-down and bottom-up techniques to form new structural motifs with high complexity. A) Hierarchical particle in particle systems, B) Pickering emulsions with anisotropic particles, and C) 3D printing of shape-defined particles, fibers, or droplets. Inset images reproduced with permission.[122] Copyright 2018, American Chemical Society. Reproduced with permission.[114] Copyright 2018, American Chemical Society, and reproduced under the terms and conditions of the Creative Commons Attribution license 4.0.[123] Copyright 2020, The Authors, published by Springer Nature.

the PLGA microparticles with confocal microscopy and electron microscopy imaging. The multiscale hierarchical nature of this drug delivery system proved to slow the burst release and control the diffusion of dexamethasone from the PLGA carrier.

Top-down and bottom-up approaches can be elegantly combined in Pickering (or particle-stabilized) emulsions. Anisotropic particles are less well explored in Pickering emulsions, mainly due to the difficulty in their synthesis, but can offer new and unusual emulsion properties including polyhedral droplets and stable larger millimeter-scale emulsions.[115–119] Kegel and co-workers investigated emulsions stabilized by cubes and peanut-shaped particles, and found that cubes arranged at the interface of oil in water emulsions in monolayers with packing densities of between 70 and 90% with domain packing intermediates between cubic and hexagonal.[120] While the peanut-shaped particles (aspect ratio 2.7) oriented parallel to their length axis with packing densities of ≈80%. Lou et al. used silica rod-shaped particles to investigate the anisotropic particle effect in emulsions with aspect ratios ranging from 1 to 16.[121] The longer particles adsorbed at the liquid/liquid interface more strongly, providing higher steric hindrance to droplet coalescence, and more stable emulsions. However, Koike et al. fabricated janus disk particles with various shapes (circular, triangular, square, pentagonal, and hexagonal) and found that they could form stable emulsions with droplet sizes in the region of 100 μm.[122] Interestingly, with very small droplet sizes, the shape of the Pickering emulsifier particles determined the shape of the droplet, due to the tessellation of the particles, and thus regular polyhedrals could be obtained.

Another recent research direction which combines both approaches to material morphology control, involves the 3D printing of droplets, fibers, or other bottom-up structures. This is particularly innovative because it allows the forming of

dexamethasone containing 200 nm spherical polymeric nanoparticles, and also free dexamethasone.[114] Both the molecular and nanoparticle cargos were found to be distributed evenly through

patterns and structures with individual compartmentalized self-assembled structures, which would not normally have long range order. Use of top-down 3D printing can allow specific networks to be formed, in a way that mimics naturally occurring networks in biological tissues. Indeed, the Bayley group, and Mann group have pioneered these methods by assembling protocells to form synthetic tissues with complex multiscale networks capable of signal transduction with electrical or biochemical cues.[123–125] Hydrogel microparticles have also been assembled into responsive networks, and 3D printed into tissue-like materials with mechanical properties comparable with those of natural tissues.[126,127] An elegant example discussed in Section 2 of this review, involved the bottom-up assembly of PAs, combined with 3D printing of these peptide nanofiber hydrogels. Top-down structure formation with the fibers allowed formation of different regions of functionality and directed growth of neuronal cell networks in vitro.[48] Strategies toward hierarchical systems involving self-assembly and nanoscale morphology control have been proposed by Ariga and co-workers.[128,129] In this case, the proposed nanoarchitectonics concept aims to create a functional material system from nanoscale units by integrating materials fabrication and potentially also additional biological components. There has been elegant uses of these nanoarchitected materials in the regulation of cell behavior through their interfacial contacts.[128,130]

5. Conclusions

Precise control over the size and shape of polymer materials is important for the use of these systems in biomedical applications. Morphology can impact various aspects of the interaction between synthetic materials and biological systems including: biodistribution, vascular wall margination, and the modulation of immune system response. This review has compared bottom-up synthesis approaches, including emulsions and emulsion polymerizations, the self-assembly of amphiphiles under specific solvent/temperature/pH or salt conditions, and biomedical applications of PISA. Top-down approaches, such as template-based lithography techniques, flow lithography methods, and 3D-printing-based methods have also been summarized. A number of recent examples combining both top-down and bottom-up methods to arrive at materials with unique properties have been highlighted. Advances in synthetic methods have allowed access to new anisotropic particles and has helped drive this research. In the future, we believe there are great opportunities to expand research combining these approaches in new ways to access multicomponent or hierarchical systems. It is important to note however, successful translation of these materials into biological applications will require improvements in current scalability and cost. In this regard, 3D-printing methods and lithographic methods could be more difficult and expensive to scale-up, however, a few companies are having success in this area including Liquidia.[131] While bottom-up syntheses potentially have an easier path to translation with scalable continuous flow methods already being applied to emulsion polymerizations, PISA, and mRNA lipid nanoparticle formation.

Conflict of Interest

The authors declare no conflict of interest.

[1] M. J. Mitchell, M. M. Billingsley, R. M. Haley, M. E. Wechsler, N. A. Peppas, R. Langer, *Nat. Rev. Drug Discovery* **2020**, *20*, 101.

[2] D. S. Williams, I. A. B. Pijpers, R. Ridolfo, J. C. M. Hestvan, *J. Controlled Release* **2017**, *259*, 29.

[3] E. Blanco, H. Shen, M. Ferrari, *Nat. Biotechnol.* **2015**, *33*, 941.

[4] A. B. Cook, S. Perrier, *Adv. Funct. Mater.* **2020**, *30*, 1901001.

[5] A. K. Pearce, T. R. Wilks, M. C. Arno, R. K. O'Reilly, *Nat. Rev. Chem.* **2020**, *5*, 21.

[6] A. B. Cook, P. Decuzzi, *ACS Nano* **2021**, *15*, 2068.

[7] A. L. Palange, R. Palomba, I. F. Rizzuti, M. Ferreira, P. Decuzzi, *Mol. Ther.* **2017**, *25*, 1514.

[8] M. V. Baranov, M. Kumar, S. Sacanna, S. Thutupalli, G. van den Bogaart, *Front. Immunol.* **2021**, *11*, 607945.

[9] D. A. Canelas, K. P. Herlihy, J. M. DeSimone, *Wiley Interdiscip. Rev. Nanomed. Nanobiotechnol.* **2009**, *1*, 391.

[10] J. Mougin, C. Bourgaux, P. Couvreur, *Adv. Drug Delivery Rev.* **2021**, *172*, 127.

[11] S. Y. Khor, J. F. Quinn, M. R. Whittaker, N. P. Truong, T. P. Davis, *Macromol. Rapid Commun.* **2019**, *40*, 1800438.

[12] J. N. Israelachvili, D. John Mitchell, B. W. Ninham, *J. Chem. Soc. Faraday Trans. 2 Mol. Chem. Phys.* **1976**, *72*, 1525.

[13] S. Chen, R. Costil, F. K.-C. Leung, B. L. Feringa, *Angew. Chem. Int. Ed.* **2021**, *60*, 11604.

[14] N. Hoshyar, S. Gray, H. Han, G. Bao, *Nanomedicine* **2016**, *11*, 673.

[15] P. Decuzzi, B. Godin, T. Tanaka, S.-Y. Lee, C. Chiappini, X. Liu, M. Ferrari, *J. Controlled Release* **2010**, *141*, 320.

[16] J. D. Robertson, G. Yealland, M. OliasAvila-, L. Chierico, O. Bandmann, S. A. Renshaw, G. Battaglia, *ACS Nano* **2014**, *8*, 4650.

[17] P. Decuzzi, M. Ferrari, *Biophys. J.* **2008**, *94*, 3790.

[18] P. Decuzzi, R. Pasqualini, W. Arap, M. Ferrari, *Pharm. Res.* **2008**, *26*, 235.

[19] P. A. Lovell, F. J. Schork, *Biomacromolecules* **2020**, *21*, 4396.

[20] P. Gurnani, A. B. Cook, R. A. E. Richardson, S. Perrier, *Polym. Chem.* **2019**, *10*, 1452.

[21] P. Gurnani, C. Sanchez-Cano, K. Abraham, H. Xandri-Monje, A. B. Cook, M. Hartlieb, F. Lévi, R. Dallmann, S. Perrier, *Macromol. Biosci.* **2018**, *18*, 1800213.

[22] J. A. Champion, S. Mitragotri, *Proc. Natl. Acad. Sci.* **2006**, *103*, 4930.

[23] A. Banerjee, J. Qi, R. Gogoi, J. Wong, S. Mitragotri, *J. Controlled Release* **2016**, *238*, 176.

[24] M. Cooley, A. Sarode, M. Hoore, D. A. Fedosov, S. Mitragotri, A. S. Gupta, *Nanoscale* **2018**, *10*, 15350.

[25] M. Nowak, T. D. Brown, A. Graham, M. E. Helgeson, S. Mitragotri, *Bioeng. Transl. Med.* **2020**, *5*, 10153.

[26] T. D. Brown, N. Habibi, D. Wu, J. Lahann, S. Mitragotri, *ACS Biomater. Sci. Eng.* **2020**, *6*, 4916.

[27] A. F. Mason, N. A. Yewdall, P. L. W. Welzen, J. Shao, M. Stevendaalvan, J. C. M. Hestvan, D. S. Williams, L. K. E. A. Abdelmohsen, *ACS Cent. Sci.* **2019**, *5*, 1360.

[28] T. Lu, E. Spruijt, *J. Am. Chem. Soc.* **2020**, *142*, 2905.

[29] T. Nisisako, S. Okushima, T. Torii, *Soft Matter* **2005**, *1*, 23.

[30] T. Nisisako, T. Torii, T. Takahashi, Y. Takizawa, *Adv. Mater.* **2006**, *18*, 1152.

[31] D. Dendukuri, P. S. Doyle, *Adv. Mater.* **2009**, *21*, 4071.

[32] K. H. Ku, Y. Kim, G.-R. Yi, Y. S. Jung, B. J. Kim, *ACS Nano* **2015**, *9*, 11333.

[33] A. H. Gröschel, F. H. Schacher, H. Schmalz, O. V. Borisov, E. B. Zhulina, A. Walther, A. H. E. Müller, *Nat. Commun.* **2012**, *3*, 710.

[34] R. Erhardt, M. Zhang, A. Böker, H. Zettl, C. Abetz, P. Frederik, G. Krausch, V. Abetz, A. H. E. Müller, *J. Am. Chem. Soc.* **2003**, *125*, 3260.

[35] A. H. Gröschel, A. Walther, T. I. Löbling, F. H. Schacher, H. Schmalz, A. H. E. Müller, *Nature* **2013**, *503*, 247.

[36] J. A. Kulkarni, S. B. Thomson, J. Zaifman, J. Leung, P. K. Wagner, A. Hill, Y. Y. C. Tam, P. R. Cullis, T. L. Petkau, B. R. Leavitt, *Nanoscale* **2020**, *12*, 23959.

[37] P. F. McKay, K. Hu, A. K. Blakney, K. Samnuan, J. C. Brown, R. Penn, J. Zhou, C. R. Bouton, P. Rogers, K. Polra, P. J. C. Lin, C. Barbosa, Y. K. Tam, W. S. Barclay, R. J. Shattock, *Nat. Commun.* **2020**, *11*, 3523.

[38] X. Wang, H. Du, Z. Wang, W. Mu, X. Han, *Adv. Mater.* **2021**, *33*, 2002635.

[39] E. S. Köksal, S. Liese, I. Kantarci, R. Olsson, A. Carlson, I. Gözen, *ACS Nano* **2019**, *13*, 6867.

[40] Q. Li, C. Li, W. Mu, X. Han, *ACS Nano* **2019**, *13*, 3573.

[41] Q. Li, X. Han, *Adv. Mater.* **2018**, *30*, 1707482.

[42] Y. J. Kang, H. S. Wostein, S. Majd, *Adv. Mater.* **2013**, *25*, 6834.

[43] R. M. P. da Silva, D. Zwaagvan der, L. Albertazzi, S. S. Lee, E. W. Meijer, S. I. Stupp, *Nat. Commun.* **2016**, *7*, 11561.

[44] T. Christoff-Tempesta, Y. Cho, D.-Y. Kim, M. Geri, G. Lamour, A. J. Lew, X. Zuo, W. R. Lindemann, J. H. Ortony, *Nat. Nanotechnol.* **2021**, *16*, 447.

[45] T. D. Clemons, S. I. Stupp, *Prog. Polym. Sci.* **2020**, *111*, 101310.

[46] S. I. Stupp, T. D. Clemons, J. K. Carrow, H. Sai, L. C. Palmer, *Isr. J. Chem.* **2020**, *60*, 124.

[47] F. Tantakitti, J. Boekhoven, X. Wang, R. V. Kazantsev, T. Yu, J. Li, E. Zhuang, R. Zandi, J. H. Ortony, C. J. Newcomb, L. C. Palmer, G. S. Shekhawat, M. O. de la Cruz, G. C. Schatz, S. I. Stupp, *Nat. Mater.* **2016**, *15*, 469.

[48] A. N. Edelbrock, T. D. Clemons, S. M. Chin, J. J. W. Roan, E. P. Bruckner, Z. Álvarez, J. F. Edelbrock, K. S. Wek, S. I. Stupp, *Adv. Sci.* **2021**, *8*, 2004042.

[49] R. Freeman, M. Han, Z. Álvarez, J. A. Lewis, J. R. Wester, N. Stephanopoulos, M. T. McClendon, C. Lynsky, J. M. Godbe, H. Sangji, E. Luijten, S. I. Stupp, *Science* **2018**, *362*, 808.

[50] J. R. Wester, J. A. Lewis, R. Freeman, H. Sai, L. C. Palmer, S. E. Henrich, S. I. Stupp, *J. Am. Chem. Soc.* **2020**, *142*, 12216.

[51] Y. Geng, P. Dalhaimer, S. Cai, R. Tsai, M. Tewari, T. Minko, D. E. Discher, *Nat. Nanotechnol.* **2007**, *2*, 249.

[52] K. Zhang, H. Fang, Z. Chen, J.-S. A. Taylor, K. L. Wooley, *Bioconjugate Chem.* **2008**, *19*, 1880.

[53] C. K. Wong, A. F. Mason, M. H. Stenzel, P. Thordarson, *Nat. Commun.* **2017**, *8*, 1240.

[54] S. C. Larnaudie, J. Sanchis, T.-H. Nguyen, R. Peltier, S. Catrouillet, J. C. Brendel, C. J. H. Porter, K. A. Jolliffe, S. Perrier, *Biomaterials* **2018**, *178*, 570.

[55] R. Ridolfo, S. Tavakoli, V. Junnuthula, D. S. Williams, A. Urtti, J. C. M. Hestvan, *Biomacromolecules* **2021**, *22*, 126.

[56] R. Ridolfo, J. J. Arends, J. C. M. Hestvan, D. S. Williams, *Biomacromolecules* **2020**, *21*, 2199.

[57] S. Cao, J. Shao, Y. Xia, H. Che, Z. Zhong, F. Meng, J. C. M. Hestvan, L. K. E. A. Abdelmohsen, D. S. Williams, *Small* **2019**, *15*, 1901849.

[58] E. M. Amodel, A.-K. Rimpelä, E. Heikkinen, O. K. Kari, E. Ramsay, T. Lajunen, M. Schmitt, L. Pelkonen, M. Bhattacharya, D. Richardson, A. Subrizi, T. Turunen, M. Reinisalo, J. Itkonen, E. Toropainen, M. Casteleijn, H. Kidron, M. Antopolsky, K.-S. Vellonen, M. Ruponen, A. Urtti, *Prog. Retinal Eye Res.* **2017**, *57*, 134.

[59] E. Gardey, F. H. Sobotta, D. Haziri, P. C. Grunert, M. T. Kuchenbrod, F. V. Gruschwitz, S. Hoeppener, M. Schumann, N. Gaßler, A. Stallmach, J. C. Brendel, bioRxiv **2021**, 2021.01.26.428316.

[60] J. S. Lee, J. Feijen, *J. Controlled Release* **2012**, *161*, 473.

[61] K. Li, D. Ding, C. Prashant, W. Qin, C.-T. Yang, B. Z. Tang, B. Liu, *Adv. Healthcare Mater.* **2013**, *2*, 1600.

[62] I. Louzao, J. C. M. Hestvan, *Biomacromolecules* **2013**, *14*, 2364.

[63] Z. Wang, M. C. M. Oersvan, F. P. J. T. Rutjes, J. C. M. Hestvan, *Angew. Chem. Int. Ed.* **2012**, *51*, 10746.

[64] W. Zhao, G. Gody, S. Dong, P. B. Zetterlund, S. Perrier, *Polym. Chem.* **2014**, *5*, 6990.

[65] N. J. Warren, S. P. Armes, *J. Am. Chem. Soc.* **2014**, *136*, 10174.

[66] J. Tan, H. Sun, M. Yu, B. S. Sumerlin, L. Zhang, *ACS Macro Lett.* **2015**, *4*, 1249.

[67] S. L. Canning, G. N. Smith, S. P. Armes, *Macromolecules* **2016**, *49*, 1985.

[68] D. B. Wright, M. A. Touve, M. P. Thompson, N. C. Gianneschi, *ACS Macro Lett.* **2018**, *7*, 401.

[69] A. Blanazs, A. J. Ryan, S. P. Armes, *Macromolecules* **2012**, *45*, 5099.

[70] J.-T. Sun, C.-Y. Hong, C.-Y. Pan, *Polym. Chem.* **2013**, *4*, 873.

[71] B. Charleux, G. Delaittre, J. Rieger, F. D'Agosto, *Macromolecules* **2012**, *45*, 6753.

[72] V. Kapishon, R. A. Whitney, P. Champagne, M. F. Cunningham, R. J. Neufeld, *Biomacromolecules* **2015**, *16*, 2040.

[73] G. Wang, M. Schmitt, Z. Wang, B. Lee, X. Pan, L. Fu, J. Yan, S. Li, G. Xie, M. R. Bockstaller, K. Matyjaszewski, *Macromolecules* **2016**, *49*, 8605.

[74] A. Shahrokhinia, R. A. Scanga, P. Biswas, J. F. Reuther, *Macromolecules* **2021**, *54*, 1441.

[75] X. G. Qiao, P.-Y. Dugas, B. Charleux, M. Lansalot, E. Bourgeat-Lami, *Macromolecules* **2015**, *48*, 545.

[76] E. Yoshida, *J. Dispersion Sci. Technol.* **2020**, *41*, 763.

[77] E. Yoshida, *Colloid Polym. Sci.* **2016**, *294*, 1857.

[78] E. Yoshida, *Colloid Polym. Sci.* **2013**, *291*, 2733.

[79] H. Tanaka, K. Yamauchi, H. Hasegawa, N. Miyamoto, S. Koizumi, T. Hashimoto, *Phys. B Condens. Matter* **2006**, *385–386*, 742.

[80] S. Varlas, S. B. Lawrenson, L. A. Arkinstall, R. K. O'Reilly, J. C. Foster, *Prog. Polym. Sci.* **2020**, *107*, 101278.

[81] K.-Y. Yoon, I.-H. Lee, K. O. Kim, J. Jang, E. Lee, T.-L. Choi, *J. Am. Chem. Soc.* **2012**, *134*, 14291.

[82] E. Hinde, K. Thammasiraphop, H. T. T. Duong, J. Yeow, B. Karagoz, C. Boyer, J. J. Gooding, K. Gaus, *Nat. Nanotechnol.* **2017**, *12*, 81.

[83] C. Cao, F. Chen, C. J. Garvey, M. H. Stenzel, *ACS Appl. Mater. Interfaces* **2020**, *12*, 30221.

[84] D. B. Wright, M. T. Proetto, M. A. Touve, N. C. Gianneschi, *Polym. Chem.* **2019**, *10*, 2996.

**ADVANCED
SCIENCE NEWS**

www.advancedsciencenews.com

**ADVANCED
NANOBIOMED
RESEARCH**
Open Access

www.advnanobiomedres.com

[85] D. B. Wright, M. P. Thompson, M. A. Touve, A. S. Carlini, N. C. Gianneschi, *Macromol. Rapid Commun.* **2019**, *40*, 1800467.

[86] M. Cieslewicz, J. Tang, J. L. Yu, H. Cao, M. Zavaljevski, K. Motoyama, A. Lieber, E. W. Raines, S. H. Pun, *Proc. Natl. Acad. Sci.* **2013**, *110*, 15919.

[87] H. Sun, W. Cao, N. Zang, T. D. Clemons, G. M. Scheutz, Z. Hu, M. P. Thompson, Y. Liang, M. Vratsanos, X. Zhou, W. Choi, B. S. Sumerlin, S. I. Stupp, N. C. Gianneschi, *Angew. Chem. Int. Ed.* **2020**, *59*, 19136.

[88] T. P. T. Dao, L. Vezenkov, G. Subra, M. Amblard, M. In, J.-F. MeinsLe, F. Aubrit, M.-A. Moradi, V. Ladmiral, M. Semsarilar, *Macromolecules* **2020**, *53*, 7034.

[89] T. P. T. Dao, L. Vezenkov, G. Subra, V. Ladmiral, M. Semsarilar, *Polym. Chem.* **2021**, *12*, 113.

[90] M. N. Vu, H. G. Kelly, A. K. Wheatley, S. Peng, E. H. Pilkington, N. A. Veldhuis, T. P. Davis, S. J. Kent, N. P. Truong, *Small* **2020**, *16*, 2002861.

[91] Y. Xia, G. M. Whitesides, *Annu. Rev. Mater. Sci.* **1998**, *28*, 153.

[92] J. P. Rolland, B. W. Maynor, L. E. Euliss, A. E. Exner, G. M. Denison, J. M. DeSimone, *J. Am. Chem. Soc.* **2005**, *127*, 10096.

[93] B. Newland, C. Taplan, D. Pette, J. Friedrichs, M. Steinhart, W. Wang, B. Voit, F. P. Seib, *Nanoscale* **2018**, *10*, 8413.

[94] M. Alghamdi, F. Chierchini, D. Eigel, C. Taplan, T. Miles, D. Pette, P. B. Welzel, C. Werner, W. Wang, C. Neto, M. Gumbleton, B. Newland, *Nanoscale Adv.* **2020**, *2*, 4498.

[95] J. Key, A. L. Palange, F. Gentile, S. Aryal, C. Stigliano, D. MascoloDi, E. De Rosa, M. Cho, Y. Lee, J. Singh, P. Decuzzi, *ACS Nano* **2015**, *9*, 11628.

[96] J. A. Finbloom, Y. Cao, T. A. Desai, *Adv. NanoBiomed Res.* **2021**, *1*, 2000057.

[97] S. E. A. Gratton, P. D. Pohlhaus, J. Lee, J. Guo, M. J. Cho, J. M. Desimone, *J. Controlled Release* **2007**, *121*, 10.

[98] S. E. A. Gratton, P. A. Ropp, P. D. Pohlhaus, J. C. Luft, V. J. Madden, M. E. Napier, J. M. DeSimone, *Proc. Natl. Acad. Sci.* **2008**, *105*, 11613.

[99] M. Colasuonno, A. L. Palange, R. Aid, M. Ferreira, H. Mollica, R. Palomba, M. Emdin, M. SetteDel, C. Chauvierre, D. Letourneur, P. Decuzzi, *ACS Nano* **2018**, *12*, 12224.

[100] M. Di Francesco, R. Primavera, M. Summa, M. Pannuzzo, V. Di Francesco, D. MascoloDi, R. Bertorelli, P. Decuzzi, *J. Controlled Release* **2020**, *319*, 201.

[101] J. C. Rose, M.-TorresCámara, K. Rahimi, J. Köhler, M. Möller, L. LaporteDe, *Nano Lett.* **2017**, *17*, 3782.

[102] D. Dendukuri, D. C. Pregibon, J. Collins, T. A. Hatton, P. S. Doyle, *Nat. Mater.* **2006**, *5*, 365.

[103] D. K. Hwang, J. Oakey, M. Toner, J. A. Arthur, K. S. Anseth, S. Lee, A. Zeiger, K. J. VlietVan, P. S. Doyle, *J. Am. Chem. Soc.* **2009**, *131*, 4499.

[104] H. J. M. Wolff, J. Linkhorst, T. Göttlich, J. Savinsky, A. J. D. Krüger, L. Laportede, M. Wessling, *Lab. Chip* **2020**, *20*, 285.

[105] S. J. Shapiro, D. Dendukuri, P. S. Doyle, *Anal. Chem.* **2018**, *90*, 13572.

[106] A. J. D. Krüger, O. Bakirman, L. P. B. Guerzoni, A. Jans, D. B. Gehlen, D. Rommel, T. Haraszti, A. J. C. Kuehne, L. D. Laporte, *Adv. Mater.* **2019**, *31*, 1903668.

[107] C. Mota, S. -EspinosaCamarero, M. B. Baker, P. Wieringa, L. Moroni, *Chem. Rev.* **2020**, *120*, 10547.

[108] Q. Ge, Z. Li, Z. Wang, K. Kowsari, W. Zhang, X. He, J. Zhou, N. X. Fang, *Int. J. Extreme Manuf.* **2020**, *2*, 022004.

[109] R. P. Doherty, T. Varkevisser, M. Teunisse, J. Hoecht, S. Ketzetzi, S. Ouhajji, D. J. Kraft, *Soft Matter* **2020**, *16*, 10463.

[110] H. Ceylan, I. C. Yasa, O. Yasa, A. F. Tabak, J. Giltinan, M. Sitti, *ACS Nano* **2019**, *13*, 3353.

[111] A. Nishiguchi, F. Shima, S. Singh, M. Akashi, M. Moeller, *Biomacromolecules* **2020**, *21*, 2043.

[112] C. Licht, J. C. Rose, A. O. Anarkoli, D. Blondel, M. Roccio, T. Haraszti, D. B. Gehlen, J. A. Hubbell, M. P. Lutolf, L. LaporteDe, *Biomacromolecules* **2019**, *20*, 4075.

[113] J. C. Rose, M. Fölster, L. Kivilip, J. L. Gerardo-Nava, E. E. Jaekel, D. B. Gehlen, W. Rohlfs, L. D. Laporte, *Polym. Chem.* **2020**, *11*, 496.

[114] M. Di Francesco, R. Primavera, D. Romanelli, R. Palomba, R. C. Pereira, T. Catelani, C. Celia, L. MarzioDi, M. Fresta, D. MascoloDi, P. Decuzzi, *ACS Appl. Mater. Interfaces* **2018**, *10*, 9280.

[115] Y. Iwashita, *Curr. Opin. Colloid Interface Sci.* **2020**, *49*, 94.

[116] D. Gonzalez Ortiz, C. Pochat-Bohatier, J. Cambedouzou, M. Bechelany, P. Miele, *Engineering* **2020**, *6*, 468.

[117] F. Geyer, Y. Asaumi, D. Vollmer, H.-J. Butt, Y. Nakamura, S. Fujii, *Adv. Funct. Mater.* **2019**, *29*, 1808826.

[118] D. Chen, E. Amstad, C.-X. Zhao, L. Cai, J. Fan, Q. Chen, M. Hai, S. Koehler, H. Zhang, F. Liang, Z. Yang, D. A. Weitz, *ACS Nano* **2017**, *11*, 11978.

[119] L. Lisuzzo, T. Hueckel, G. Cavallaro, S. Sacanna, G. Lazzara, *ACS Appl. Mater. Interfaces* **2021**, *13*, 1651.

[120] J. W. J. Folterde, E. M. Hutter, S. I. R. Castillo, K. E. Klop, A. P. Philipse, W. K. Kegel, *Langmuir* **2014**, *30*, 955.

[121] F. Lou, L. Ye, M. Kong, Q. Yang, G. Li, Y. Huang, *RSC Adv.* **2016**, *6*, 24195.

[122] R. Koike, Y. Iwashita, Y. Kimura, *Langmuir* **2018**, *34*, 12394.

[123] A. Alcinesio, O. J. Meacock, R. G. Allan, C. Monico, V. Schild Restrepo, I. Cazimoglu, M. T. Cornall, R. Krishna Kumar, H. Bayley, *Nat. Commun.* **2020**, *11*, 2105.

[124] P. Gobbo, A. J. Patil, M. Li, R. Harniman, W. H. Briscoe, S. Mann, *Nat. Mater.* **2018**, *17*, 1145.

[125] M. J. Booth, V. R. Schild, A. D. Graham, S. N. Olof, H. Bayley, *Sci. Adv.* **2016**, *2*, 1600056.

[126] F. G. Downs, D. J. Lunn, M. J. Booth, J. B. Sauer, W. J. Ramsay, R. G. Klemperer, C. J. Hawker, H. Bayley, *Nat. Chem.* **2020**, *12*, 363.

[127] M. Hirsch, A. Charlet, E. Amstad, *Adv. Funct. Mater.* **2021**, *31*, 2005929.

[128] K. Ariga, K.-C. Tsai, L. K. Shrestha, S. Hsu, *Mater. Chem. Front.* **2021**, *5*, 1018.

[129] L. Zhao, Q. Zou, X. Yan, *Bull. Chem. Soc. Jpn.* **2019**, *92*, 70.

[130] J. Song, X. Jia, K. Ariga, *Mater. Today Bio* **2020**, *8*, 100075.

[131] J. M. DeSimone, *J. Controlled Release* **2016**, *240*, 541.

[132] M. Semsarilar, V. Ladmiral, A. Blanazs, S. P. Armes, *Langmuir* **2013**, *29*, 7416.

[133] A. Blanazs, J. Madsen, G. Battaglia, A. J. Ryan, S. P. Armes, *J. Am. Chem. Soc.* **2011**, *133*, 16581.

[134] P. Yang, L. P. D. Ratcliffe, S. P. Armes, *Macromolecules* **2013**, *46*, 8545.

[135] W.-J. Zhang, C.-Y. Hong, C.-Y. Pan, *Macromolecules* **2014**, *47*, 1664.

[136] W.-M. Wan, C.-Y. Pan, *Macromolecules* **2010**, *43*, 2672.

ADVANCED
SCIENCE NEWS
www.advancedsciencenews.com

ADVANCED
NANOBIOMED
RESEARCH
Open Access
www.advnanobiomedres.com

Alexander B. Cook is a Marie Curie Fellow at the Eindhoven University of Technology with Professor Jan van Hest. Previously, he worked with Professor Paolo Decuzzi at the Italian Institute of Technology, and spent a period as scientist at the biotech eTheRNA Immunotherapies. He has a Ph.D. in chemistry from the University of Warwick where he worked on branched polymer architectures for RNA delivery.

Tristan D. Clemons earned a B.Sc. in chemistry from Curtin University and a Ph.D. from the University of Western Australia under the supervision of Professor Iyer Swaminathan investigating polymeric nanoparticles for therapeutic delivery. He is currently an assistant professor at the University of Southern Mississippi within the School of Polymer Science and Engineering. The research interests of the Clemons Lab focus on polymers, both covalent and supramolecular, for biomedical applications.